



Article

# Design, Synthesis, and Biological Evaluations of Novel Azothiazoles Based on Thioamide

Abdelwahed R. Sayed<sup>1,2,\*</sup>, Hany Elsayy<sup>1,3</sup> , Saad Shaaban<sup>1,4</sup>, Sobhi M. Gomha<sup>5,6</sup> and Yasair S. Al-Faiyz<sup>1</sup>

<sup>1</sup> Department of Chemistry, Faculty of Science, King Faisal University, P.O. Box 380, Hofuf 31982, Saudi Arabia; hmostafa@kfu.edu.sa (H.E.); sbrahim@kfu.edu.sa (S.S.); yalfayz@kfu.edu.sa (Y.S.A.-F.)

<sup>2</sup> Department of Chemistry, Faculty of Science, Beni-Suef University, Beni-Suef 62514, Egypt

<sup>3</sup> Department of Chemistry, Faculty of Science, Tanta University, Tanta 31111, Egypt

<sup>4</sup> Organic Chemistry Division, Chemistry Department, Faculty of Science, Mansoura University, Mansoura 35516, Egypt

<sup>5</sup> Department of Chemistry, Faculty of Science, Cairo University, Giza 12613, Egypt; s.m.gomha@gmail.com

<sup>6</sup> Department of Chemistry, Faculty of Science, Islamic University in Almadinah Almonawara, Almadinah Almonawara 42351, Saudi Arabia

\* Correspondence: arsayed@kfu.edu.sa; Tel.: +966-561-009-338

**Abstract:** Herein we studied the preparation of different thiazoles via the reaction of 2-(3,4-dimethoxybenzylidene)hydrazine-1-carbothioamide (**1**) with hydrazonoyl halides under base-catalyzed conditions. The reactions proceed through nucleophilic substitution attack at the halogen atom of the hydrazonoyl halides by the thiol nucleophile to form an *S*-alkylated intermediate. The latter intermediate undergoes cyclization by the loss of water to afford the final products. The structures of the azo compounds were confirmed by FTIR, MS, NMR, and elemental analyses. Indeed, the newly synthesized azo compounds were estimated for their potential anticancer activities by an MTT assay against different human cancer cells, such as lung adenocarcinoma (A549) and colorectal adenocarcinoma (DLD-1). The caspase-3 levels were also estimated using Western blotting and the dual staining technique to evaluate the potency of the titled compounds to promote apoptosis.

**Keywords:** thiazole; hydrazonoyl; carbothioamide; anticancer activities



**Citation:** Sayed, A.R.; Elsayy, H.; Shaaban, S.; Gomha, S.M.; Al-Faiyz, Y.S. Design, Synthesis, and Biological Evaluations of Novel Azothiazoles Based on Thioamide. *Curr. Issues Mol. Biol.* **2022**, *44*, 2956–2966. <https://doi.org/10.3390/cimb44070204>

Academic Editor: Hidayat Hussain

Received: 28 May 2022

Accepted: 27 June 2022

Published: 1 July 2022

**Publisher's Note:** MDPI stays neutral with regard to jurisdictional claims in published maps and institutional affiliations.



**Copyright:** © 2022 by the authors. Licensee MDPI, Basel, Switzerland. This article is an open access article distributed under the terms and conditions of the Creative Commons Attribution (CC BY) license (<https://creativecommons.org/licenses/by/4.0/>).

## 1. Introduction

Azo dyes have attracted much attention owing to their outstanding biological and physicochemical properties and diverse applications in different aspects of life, such as analytical chemistry, pharmaceuticals, cosmetics, painting, and the dyeing industry [1–3]. Furthermore, they are easily accessible, relatively stable, and manifest various pharmacological applications (e.g., anticancer, antimicrobial, and antiviral activities) [3–5]. Indeed, they are also used in targeted therapy as prodrugs and drug delivery in the case of colitis [6]. Despite being toxic to the environment and humans, many efforts are oriented to modify their structures and improve their biological profiles [7–11].

On the other hand, thiazoles are prepared from the reaction hydrazones with different hydrazonoyl halides [12,13]. They were intensively investigated for their anticancer activities and DNA-binding abilities [14,15]. Moreover, bithiazoles were prepared from the reaction of bishydrazones with different types of haloketone and were also studied as bioactive skeletons [16]. The goal of this work was to develop novel azothiazoles from the reaction of different hydrazonoyl halides with 2-(3,4-dimethoxybenzylidene)hydrazine-1-carbothioamide (**1**). The final prepared compounds were elucidated by FTIR, MS, NMR, and elemental analyses. Their potential anticancer activities were estimated by MTT assays and their potency to promote apoptosis was estimated with caspase-3 assays.

## 2. Materials and Methods

### 2.1. Synthesis

#### 2.1.1. General Information

The materials were obtained from Fluka and Aldrich. All materials were used without further purification. We checked the melting points by using a Gallen Kamp thermoelectric temperature device. The  $^1\text{H}$  and  $^{13}\text{C}$  NMR spectra were verified in deuterated-dimethylsulfoxide with tetramethyl-silane as an internal average via a spectrometer (Varian Gemini 300 MHz). Infrared spectra were investigated via potassium bromide wafer on Pye Unicam, and a Fourier transform infrared spectrophotometer. Elemental microanalyses were done in the micro-analytical laboratory at the University of Cairo, Giza, Egypt.

#### 2.1.2. General Procedure for the Synthesis of Azothiazole Derivatives (8–13) and (17–19)

Treatment of 2-(3,4-dihydroxybenzylidene)hydrazine-1-carbothioamide **1** (10 mmol) with other hydrazonoyl chloride **2–7** (10 mmol) or bishydrazonoyl halides **14–16** (5 mmol) was in the presence of an equivalent molar ratio of a basic catalyst such as triethylamine in 15 mL of dioxane. The reaction mixtures were heated under reflux for 6 h, and the solvent was distilled off under reduced pressure. The solid was crystallized from an appropriate solvent and dried at 75 °C for 48 h.

#### 2-(2-(3,4-Dimethoxybenzylidene)hydrazinyl)-5-methyl-4-(phenyldiazenyl)thiazole **8**

Red orange solid (74%); mp. 128–130 °C; IR (KBr):  $\nu$  3188 (NH), 1595 (C=N)  $\text{cm}^{-1}$ .  $^1\text{H}$  NMR (DMSO- $d_6$ ): 2. 61 (s, 3H, CH<sub>3</sub>), 3.81 (s, 3H, CH<sub>3</sub>), 3.84 (s, 3H, CH<sub>3</sub>), 7.15–7.77 (m, 8H, ArH), 8.59 (s, 1H, N=CH) and 10.81 (s, 1H, NH) ppm. MS  $m/z$  (%): 381 ( $\text{M}^+$ , 26). Anal. Calcd. for C<sub>19</sub>H<sub>19</sub>N<sub>5</sub>O<sub>2</sub>S (381.13): C, 59.83; H, 5.02; N, 18.36; Found C, 59.71; H, 5.23; N, 18.44%.

#### 2-(2-(3,4-Dimethoxybenzylidene)hydrazinyl)-5-methyl-4-(p-tolyldiazenyl)thiazole **9**

Red orange solid (84%); mp. 140–141 °C; IR (KBr):  $\nu$  3196 (NH), 1609 (C=N)  $\text{cm}^{-1}$ .  $^1\text{H}$  NMR (DMSO- $d_6$ ): 2. 31 (s, 3H, CH<sub>3</sub>), 2. 59 (s, 3H, CH<sub>3</sub>), 3.81 (s, 3H, CH<sub>3</sub>), 3.83 (s, 3H, CH<sub>3</sub>), 7.08–7.69 (m, 7H, ArH), 8.91 (s, 1H, N=CH) and 10.74 (s, 1H, NH) ppm. MS  $m/z$  (%): 395 ( $\text{M}^+$ , 21). Anal. Calcd. for C<sub>20</sub>H<sub>21</sub>N<sub>5</sub>O<sub>2</sub>S (395.48): C, 60.74; H, 5.35; N, 17.71; Found C, 60.70; H, 5.64; N, 17.42%.

#### 4-((2-(2-(3,4-Dimethoxybenzylidene)hydrazinyl)-5-methylthiazol-4-yl)diazenyl)benzenesulfonic acid **10**

Red orange solid (77%); mp. 225–227 °C; IR (KBr):  $\nu$  3299 (NH), 1601 (C=N)  $\text{cm}^{-1}$ .  $^1\text{H}$  NMR (DMSO- $d_6$ ): 2. 59 (s, 3H, CH<sub>3</sub>), 3.81 (s, 3H, CH<sub>3</sub>), 3.83 (s, 3H, CH<sub>3</sub>), 6.96–7.58 (m, 7H, ArH), 8.41 (s, 1H, N=CH), 8.92 (s, 1H, SO<sub>3</sub>H) and 10.67 (s, 1H, NH) ppm.  $^{13}\text{C}$  NMR (DMSO- $d_6$ ): at 16.47, 55.53, 55.67, 110.04, 113.11, 123.26, 126.43, 126.76, 138.34, 142.28, 143.39, 148.95, 152.05, 160.29 and 171.45 ppm. MS  $m/z$  (%): 461 ( $\text{M}^+$ , 42). Anal. Calcd. for C<sub>19</sub>H<sub>19</sub>N<sub>5</sub>O<sub>5</sub>S<sub>2</sub> (461.08): C, 49.45; H, 4.15; N, 15.18; Found C, 49.32; H, 4.11; N, 15.29%.

#### 1-(4-((2-(2-(3,4-Dimethoxybenzylidene)hydrazinyl)-5-methylthiazol-4-yl)diazenyl)phenyl)ethan-1-one **11**

Red brown solid (79%); mp. 240–242 °C; IR (KBr):  $\nu$  3322 (NH), 1684 (C=O), 1601 (C=N)  $\text{cm}^{-1}$ .  $^1\text{H}$  NMR (DMSO- $d_6$ ): 2.73 (s, 3H, CH<sub>3</sub>), 3.06 (s, 3H, CH<sub>3</sub>), 3.81 (s, 3H, CH<sub>3</sub>), 3.84 (s, 3H, CH<sub>3</sub>), 7.31–7.92 (m, 7H, ArH), 8.61 (s, 1H, N=CH) and 10.73 (s, 1H, NH) ppm. MS  $m/z$  (%): 423 ( $\text{M}^+$ , 22). Anal. Calcd. for C<sub>21</sub>H<sub>21</sub>N<sub>5</sub>O<sub>3</sub>S (423.14): C, 59.56; H, 5.00; N, 16.54; Found C, 59.71; H, 5.12; N, 16.41%.

#### 3-((2-(2-(3,4-Dimethoxybenzylidene)hydrazinyl)-5-methylthiazol-4-yl)diazenyl)phenol **12**

Deep red solid (88%); mp. 200–201 °C; IR (KBr):  $\nu$  3349 (OH), 3262 (NH), 1591 (C=N)  $\text{cm}^{-1}$ .  $^1\text{H}$  NMR (DMSO- $d_6$ ): 2. 56 (s, 3H, CH<sub>3</sub>), 3. 81 (s, 3H, CH<sub>3</sub>), 3.84 (s, 3H, CH<sub>3</sub>), 6.72–7.97 (m, 7H, ArH), 8.17 (s, 1H, N=CH), 9.65 (s, 1H, OH), and 11.33 (s, 1H, NH) ppm.

$^{13}\text{C}$  NMR (DMSO- $d_6$ ): at 26.46; 55.47; 55.62; 108.41; 111.16; 115.75; 116.05; 120.18; 122.15; 129.88; 132.06; 133.67; 146.33; 149.10; 150.54; 155.85 and 177.45 ppm. MS  $m/z$  (%): 397 ( $\text{M}^+$ , 33). Anal. Calcd. for  $\text{C}_{19}\text{H}_{19}\text{N}_5\text{O}_3\text{S}$  (397.12): C, 57.42; H, 4.82; N, 17.62; Found C, 57.31; H, 4.70; N, 17.81%.

2-(2-(3,4-Dimethoxybenzylidene)hydrazinyl)-5-methyl-4-((2-nitrophenyl)diazenyl)thiazole **13**

Deep red solid (68%); mp. 220–222 °C, IR (KBr):  $\nu$  3299 (NH), 1605 (C=N)  $\text{cm}^{-1}$ .  $^1\text{H}$  NMR (DMSO- $d_6$ ): 2. 59 (s, 3H,  $\text{CH}_3$ ), 3. 81 (s, 3H,  $\text{CH}_3$ ), 3.84 (s, 3H,  $\text{CH}_3$ ), 7.11–7.87 (m, 7H, ArH), 8.65 (s, 1H, N=CH) and 10.99 (s, 1H, NH) ppm. MS  $m/z$  (%): 426 ( $\text{M}^+$ , 23). Anal. Calcd. for  $\text{C}_{19}\text{H}_{18}\text{N}_6\text{O}_4\text{S}$  (426.45): C, 53.51; H, 4.25; N, 19.71; Found C, 53.33; H, 4.25; N, 19.94%.

4,4'-((Sulfonylbis(4,1-phenylene))bis(diazene-2,1-diyl))bis(2-(2-(3,4-dimethoxybenzylidene)hydrazinyl)-5-methylthiazole) **17**

Red solid (81%); mp. 235–236 °C, IR (KBr):  $\nu$  3368 (NH), 1593 (C=N)  $\text{cm}^{-1}$ .  $^1\text{H}$  NMR (DMSO- $d_6$ ): 2. 59 (s, 6H, 2 $\text{CH}_3$ ), 3. 81 (s, 6H, 2 $\text{CH}_3$ ), 3. 83 (s, 6H, 2 $\text{CH}_3$ ), 7.11–7.88 (m, 14H, ArH), 8.59 (s, 2H, N=CH) and 9.73 (s, 2H, NH) ppm.  $^{13}\text{C}$  NMR (DMSO- $d_6$ ): at 25.57, 55.52, 55.67, 109.98, 111.64, 123.38, 128.17, 128.93, 129.32, 133.82, 135.14, 140.74, 147.98, 148.95, 152.09, 160.48 and 177.69. MS  $m/z$  (%): 824 ( $\text{M}^+$ , 17). Anal. Calcd. for  $\text{C}_{38}\text{H}_{36}\text{N}_{10}\text{O}_6\text{S}_3$  (824.20): C, 55.33; H, 4.40; N, 16.98; Found C, 55.27; H, 4.51; N, 16.79%.

1,4-Bis((2-(2-(3,4-dimethoxybenzylidene)hydrazinyl)-5-methylthiazol-4-yl)diazenyl)benzene **18**

Deep red solid (79%); mp. > 300 °C, IR (KBr):  $\nu$  3252 (NH), 1601 (C=N)  $\text{cm}^{-1}$ .  $^1\text{H}$  NMR (DMSO- $d_6$ ): 2. 61 (s, 6H, 2 $\text{CH}_3$ ), 3.81 (s, 6H, 2 $\text{CH}_3$ ), 3.85 (s, 6H, 2 $\text{CH}_3$ ), 7.12–7.86 (m, 10H, ArH), 8.61 (s, 2H, N=CH) and 10.71 (s, 2H, NH) ppm. MS  $m/z$  (%): 684 ( $\text{M}^+$ , 28). Anal. Calcd. for  $\text{C}_{32}\text{H}_{32}\text{N}_{10}\text{O}_4\text{S}_2$  (684.20): C, 56.13; H, 4.71; N, 20.45; Found C, 56.21; H, 4.56; N, 20.59%.

1,3-Bis((2-(2-(3,4-dimethoxybenzylidene)hydrazinyl)-5-methylthiazol-4-yl)diazenyl)benzene **19**

Deep red solid (80%); mp. > 300 °C, IR (KBr):  $\nu$  3196 (NH), 1593 (C=N)  $\text{cm}^{-1}$ .  $^1\text{H}$  NMR (DMSO- $d_6$ ): 2.62 (s, 6H, 2 $\text{CH}_3$ ), 3.82 (s, 6H, 2 $\text{CH}_3$ ), 3.85 (s, 6H, 2 $\text{CH}_3$ ), 7.01–7.48 (m, 10H, ArH), 8.59 (s, 2H, N=CH) and 10.71 (s, 2H, NH) ppm. MS  $m/z$  (%): 684 ( $\text{M}^+$ , 34). Anal. Calcd. for  $\text{C}_{32}\text{H}_{32}\text{N}_{10}\text{O}_4\text{S}_2$  (684.20): C, 56.13; H, 4.71; N, 20.45; Found C, 56.29; H, 4.95; N, 20.24%.

## 2.2. Biological Evaluations

### 2.2.1. Cell Culture and MTT Assay

The colon cancer cell lines (DLD-1) and non-small lung cancer cell lines (A549) were plated separately using 96-well plates with a concentration of  $1 \times 10^4$  cells/well in DMEM media with  $1 \times$  Antibiotic Antimycotic Solution and 10% fetal bovine serum (Himedia, Mumbai, India) in a  $\text{CO}_2$  incubator at 37 °C with 5%  $\text{CO}_2$ . First, the cells were washed with 200  $\mu\text{L}$  of  $1 \times$  PBS, and then the cells were treated with Samples **1–11** (10–100  $\mu\text{M}/\text{mL}$ ) with various test concentrations of a compound in serum-free media and incubated for 24 h. The medium was aspirated from cells at the end of the treatment period. Next, 0.5 mg/mL MTT prepared in  $1 \times$  PBS was added and incubated at 37 °C for 4 h using a  $\text{CO}_2$  incubator. After incubation, the medium containing MTT was discarded from the cells and washed using 200  $\mu\text{L}$  of PBS. The formed crystals were dissolved with 100  $\mu\text{L}$  of DMSO and thoroughly mixed. The development of color intensity was evaluated at 570 nm. The formazan dye turns to purple-blue color. The absorbance was measured at 570 nm using a microplate reader.

### 2.2.2. Immunoblotting

After treatment with different samples on the DLD-1 and A549 cell lines for 24 h, cells were harvested using trypsin and washed twice with ice-cold PBS. For immunoblotting analysis, cells were lysed in RIPA buffer (Sana crus, Biotech, Dallas, TX, USA) for 14 min on ice, and then centrifuged at  $8000\times g$  for 15 min at 4 °C. Supernatants were collected and estimated using a Bradford assay. A total of 250 µg protein was denatured at 92 °C for 7 min. Equal amounts of protein were then separated on SDS-PAGE gels and transferred to PVDF membranes. Membranes were blocked with 5% nonfat milk at room temperature for 30 h and incubated with primary antibodies (Caspase-3 (1:2000), Cell Signaling Technology (CST; Beverly, MA, USA) overnight at 4 °C, and then with a horseradish peroxidase-conjugated secondary antibody at room temperature for 1 h. Protein bands were visualized by enhanced chemiluminescence (Licor analyzer). B-actin was used as an internal control.

### 2.2.3. DUAL Staining

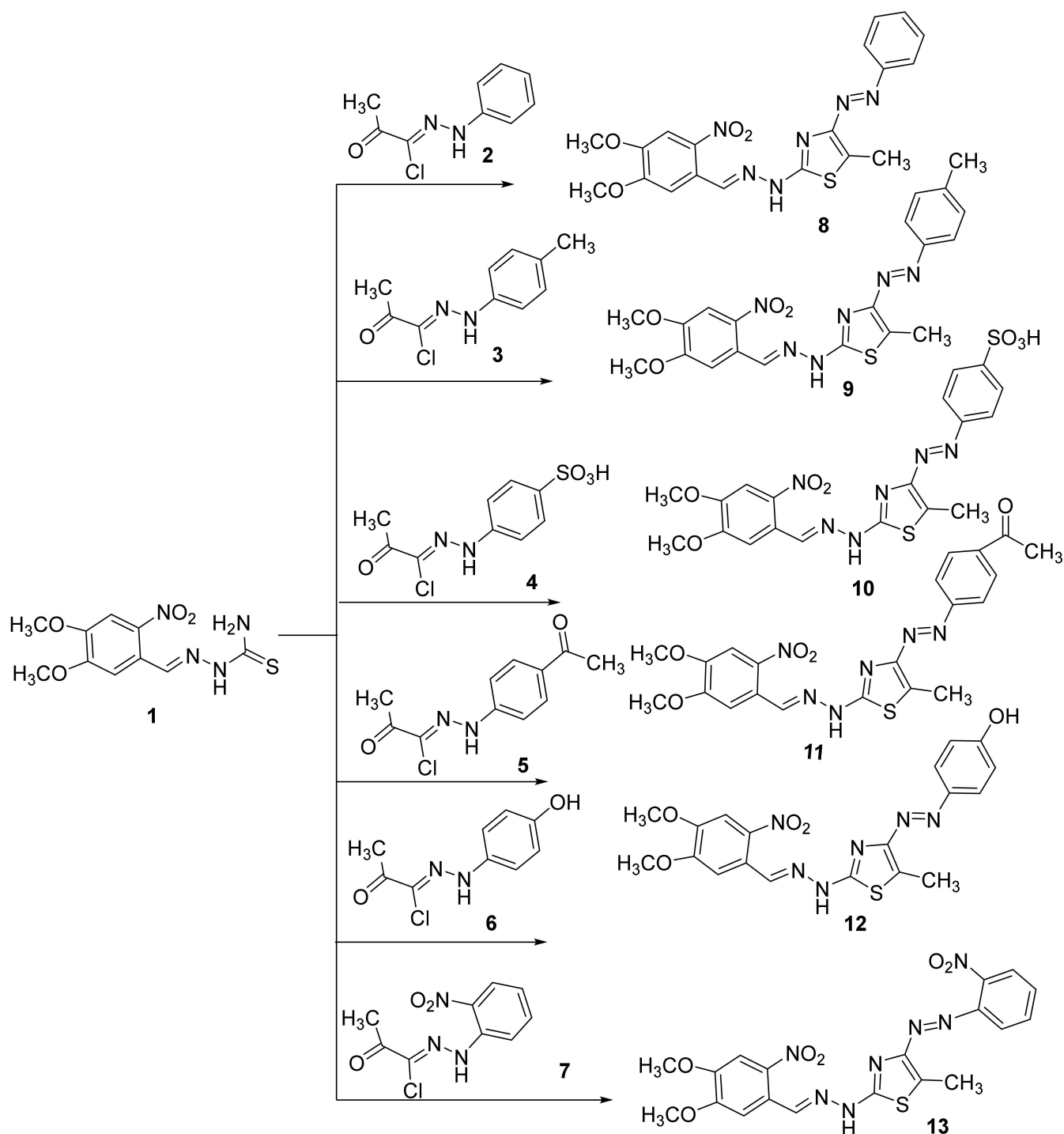
Dual AO/EB fluorescent staining: After 12 h the treated cells were obtained in 12-well plates, human colon cancer cells and lung cancer cells (DLD-1 and A549), respectively, at the logarithmic growth phase, and cells were washed using ice-cold PBS. Dual fluorescent staining solution (1 µL) containing 100 µg/mL AO and 100 µg/mL EB (AO/EB, Sigma, St. Louis, MO, USA) was added to each suspension, and excess stains were removed. The morphology of apoptotic cells was examined, and 100 cells were counted within 20 min using a fluorescent microscope (Leica, Italy). The dual acridine orange/ethidium bromide (AO/EB) staining method was repeated three times at least. The fluorescence was recorded by Image J software, and values are expressed as fold changes.

Statistics: All statistical analyses were performed using the GraphPad 14.0 software for Windows. A *p*-value of <0.05 was considered statistically significant.

## 3. Results

### 3.1. Chemistry

Recently, we reported several hydrazoneyl halides and their utility in synthesizing several heterocyclics [17–24]. Herein we focused on developing novel mono and bisazothiazoles. The reaction of 2-(3,4-dihydroxybenzylidene)hydrazine-1-carbothioamide (**1**) with  $\alpha$ -haloketohydrazoneyl halides **2–7** in a suitable solvent in the presence of base catalyst under heating afforded the corresponding azothiazoles **8–13** (Scheme 1). The explanation of the reaction can be through a nucleophilic substitution reaction that starts with the halogen atom from hydrazoneyl halides being replaced by the thiol nucleophile of 2-(3,4-dimethoxybenzylidene)hydrazine-1-carbothioamide to form an *S*-alkylated intermediate. This intermediate could undergo cyclization carried out via nucleophilic addition followed by the loss of water, which would afford the final products. All reactions are given in every example, one product, as observed by TLC. Interestingly, all compounds were prepared in good yields (up to 88%). The final products of the isolated thiazoles **8–13** were elucidated using elemental analysis and different spectral technics. For instance, the IR spectrum of the synthesized thiazoles **8–13** displayed an absorption peak near  $3188\text{--}3299\text{ cm}^{-1}$  for the NH.

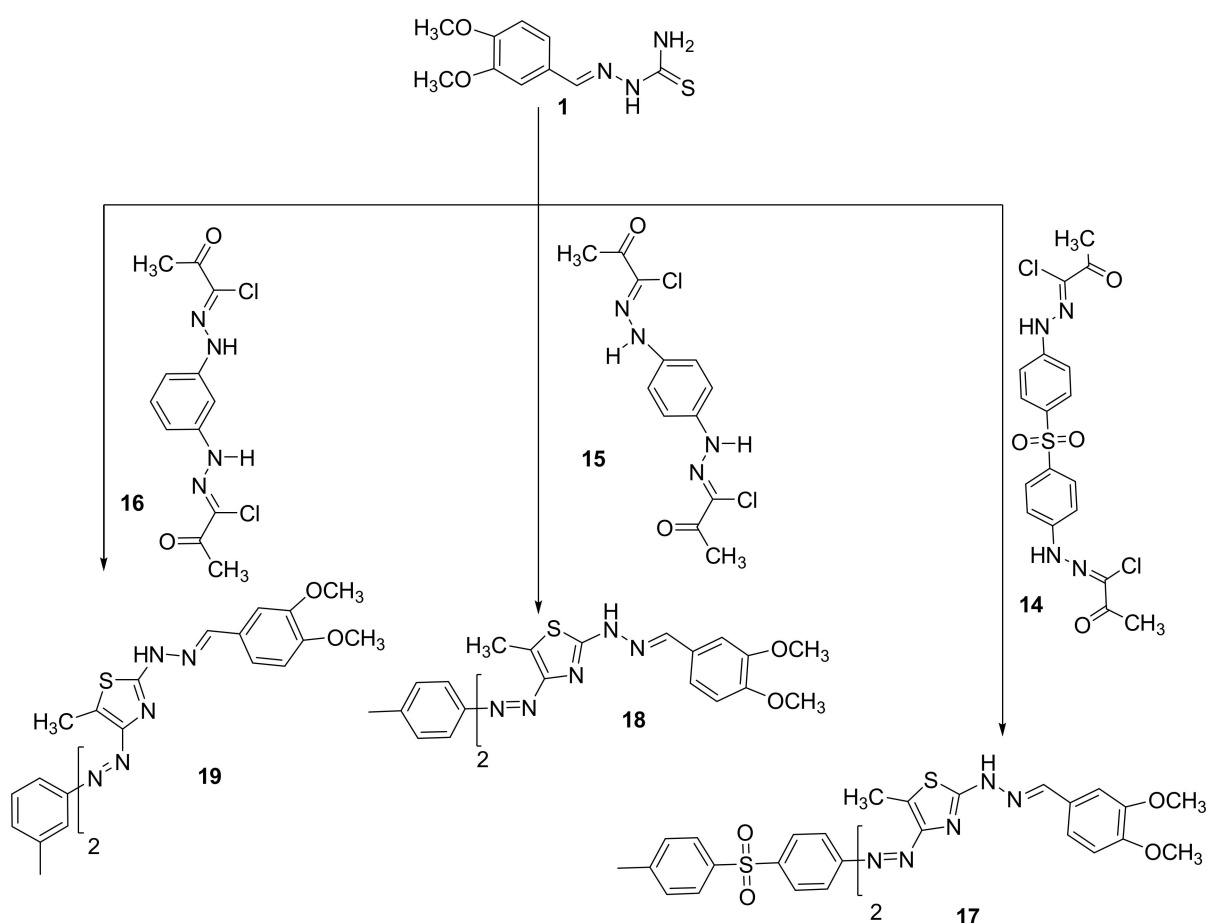


**Scheme 1.** Synthesis of monoazothiazoles 8–13.

Furthermore, we found in the final products 8–13 disappearance of C=O, which is present in the starting compounds 2–7. All thiazoles 8–13 showed the expected molecular ion peaks at the correct  $m/z$  values. Additionally,  $^1\text{H}$  NMR spectra of 8–13 showed all protons as expected from the proposed structure, as shown in Scheme 1. The  $^{13}\text{C}$  NMR for the final products could not be obtained due to poor solubility of most of the compounds, except for compounds 10 and 12 (see experimental part).

The bisazothiazoles were also prepared from the reaction of 2-(4,5-dimethoxy-2-nitrobenzylidene)hydrazine-1-carbothioamide (1) with bishydrazonoyl chloride 14–16 in

Et<sub>3</sub>N/dioxane (Scheme 2). The reactions proceeded through nucleophilic substitution reaction that starts with the halogen atom from bishydrazonoyl halides being replaced by the thiol nucleophile of 2-(3,4-dimethoxybenzylidene)hydrazine-1-carbothioamide (**1**) to form an S-alkylated intermediate. This intermediate could undergo cyclization carried out via nucleophilic addition followed by the loss of water, which would afford the final products **17–19**, as described in Scheme 2. The novel bisazothiazoles were characterized according by different spectral analysis. For example, the IR spectrum of the synthesized thiazoles **17–19** displayed an absorption peak near 3196–3368 cm<sup>-1</sup> for the NH. Furthermore, we found in the final products **17–19** the disappearance of C=O, which is present in the start compounds **2–6**. All thiazoles **17–19** have shown the expected molecular ion peaks at the foreseeable *m/z* values. Additionally, in the <sup>1</sup>H NMR spectra of **17–19** are shown all the protons that were tailored with the proposed structure as shown in Scheme 2. <sup>13</sup>CNMR for the final products could not appear due to poor solubility, except for compound **17** (see experimental part).



**Scheme 2.** Synthesis of bisazothiazoles **17–19**.

### 3.2. Biology

#### 3.2.1. Cytotoxicity

The azo group is a common functionality in many interesting organic compounds with different applications (e.g., painting, ink, staining of biological systems, and LCD) and potential medicinal activities (e.g., antitumor and antimicrobial) [25–28]. Furthermore, the anticancer activities of the azo compounds have been reported in numerous reports due to their potency to intercalate with RNA and/or DNA, as well as the inhibition of various proteins [3–5,11]. In this regard, the antitumor activities of the novel azo compounds were

assessed against the lung A549 and colorectal DLD-1 adenocarcinomas via an MTT assay, and the IC<sub>50</sub> values are shown in Table 1.

**Table 1.** Effect of the synthesized compounds on the viability of human colorectal adenocarcinoma (DLD-1) and human adenocarcinoma(A549) cells.

Compounds	IC <sub>50</sub> (μM) <sup>a</sup>	
	A549	DLD-1
Cisplatin	6 ± 1.2	7.3 ± 2.6
8	42 ± 3.7	26 ± 2.7
9	- <sup>b</sup>	- <sup>b</sup>
10	- <sup>b</sup>	- <sup>b</sup>
11	40 ± 3.83	21 ± 1.6
12	23 ± 2.9	32 ± 2.9
13	32 ± 4.1	35 ± 4.21
17	- <sup>b</sup>	- <sup>b</sup>
18	- <sup>b</sup>	43
19	- <sup>b</sup>	- <sup>b</sup>

<sup>a</sup> Cytotoxicity was measured after forty-eight hours treatment of DLD-1 and A549 cells with serial concentrations of the newly synthesized compounds using an MTT assay. <sup>b</sup> No proliferation inhibition (IC<sub>50</sub> ≥ 50) was observed at the tested concentration range.

In general, most of the azo compounds showed superior cytotoxicity to the DLD-1 compared to the A549. In the case of DLD-1, azo agents 8 and 11 were the most cytotoxic, with IC<sub>50</sub>s of 26 ± 2.7 and 21 ± 1.6 μM, respectively, whereas compounds 12 and 13 showed moderate anticancer activity, with IC<sub>50</sub>s of 32 ± 2.9 and 35 ± 4.21 μM, respectively. In the case of A549 cells, azo compound 12 was the most cytotoxic, with an IC<sub>50</sub> of 23 ± 2.9 μM. Furthermore, compounds 8, 11, and 13 were the least active, with IC<sub>50</sub>s of 42 ± 3.7, 40 ± 3.83, and 32 ± 4.1 μM, respectively. Collectively, the most cytotoxic compounds were further selected for further biological investigations.

### 3.2.2. Caspase Activity

Caspases are among the proteases involved in apoptosis induction [28]. In particular, caspase-3 is an effector caspase enrolled in the apoptosis execution final stage [4,29]. Accordingly, caspase-3 activation is routinely estimated by medicinal chemists to evaluate the apoptosis as an indication [30,31]. Therefore, the caspase-3 levels were assessed in A549 and DLD-1 cells employing Western blotting, as presented in Figure 1.

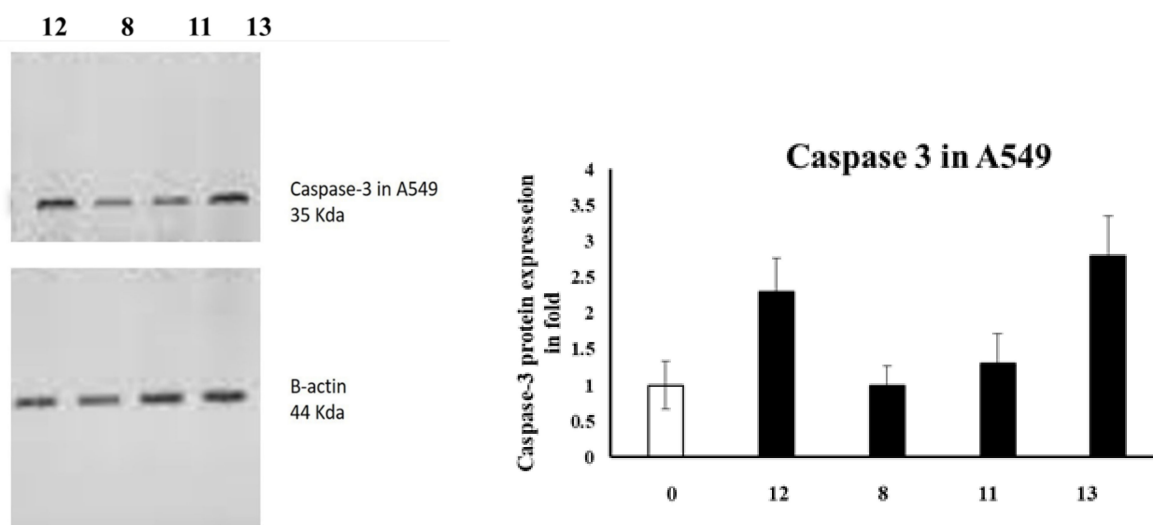


**Figure 1.** Cont.

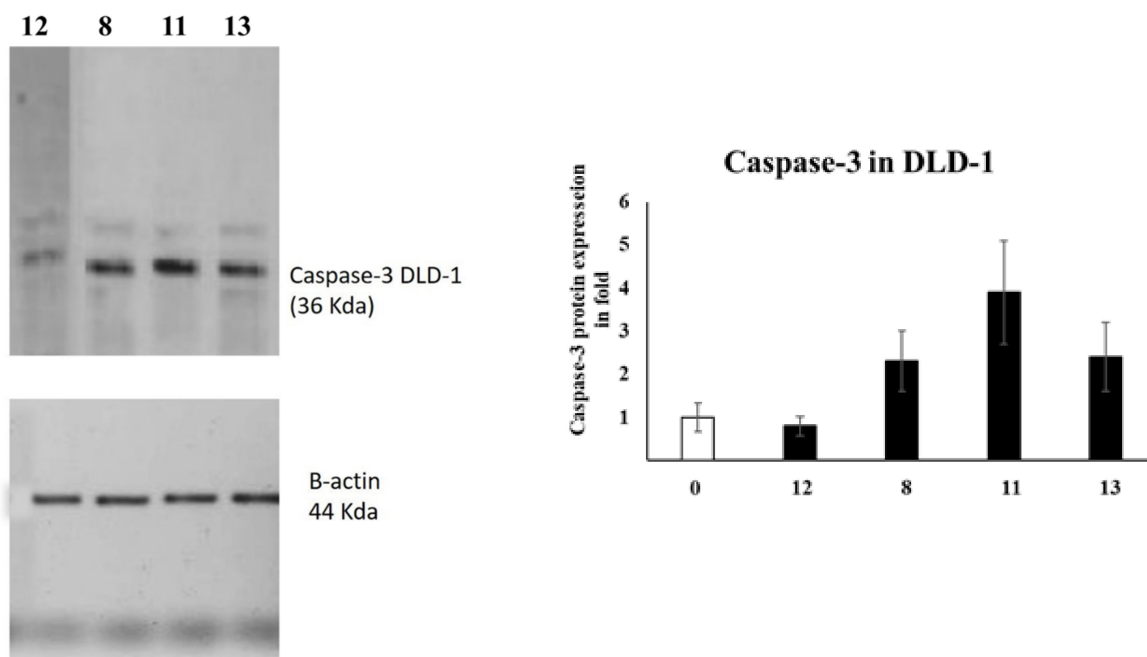


**Figure 1.** The levels of Caspase-3 in A5941 and DLD-1 cells of various groups were examined by Western blotting.

In the case of DLD-1 cells, azo compound **11** was the most active and upregulated caspase-3 expression by 4-fold compared to the negative (untreated) control. Furthermore, compound **13** could also activate caspase-3 expression up to 3-fold compared to the negative control.

In the case of A549 cells, azo compound **13** upregulated caspase-3 expression by 3.5-fold compared to the untreated control, whereas azo compound **12** was only able to activate caspase-3 expression up to 2.5-fold compared to the negative control.

To conclude, our experiments showed that the caspase-3 levels were activated in DLD-1 and A549 cells, which might promote apoptosis and lead to cell death.

### 3.2.3. Dual AO/EB Fluorescent Staining

It is worth noting that various cell morphology alterations accompany apoptosis. Such hallmarks include the formation of cytoplasmic blebs, chromatin condensation, and fragmentation of the nucleus [32–34]. Additionally, the shape of the cell turns to be irregular and associated with the formation of apoptotic bodies of DNA fragments as well as the size of the nucleus [32,35–41]. The novel azo dyes' anticancer properties and apoptosis induction were further evaluated using a dual staining technique via the fluorescent homidium bromide and acridine orange dyes. It is worth noting that the dual AO/EB fluorescent staining technique revealed the differences between necrotic and apoptotic cells. In this regard, it is obvious that the novel azoic dyes promote different cell morphology alterations, as shown in Figures 2 and 3.

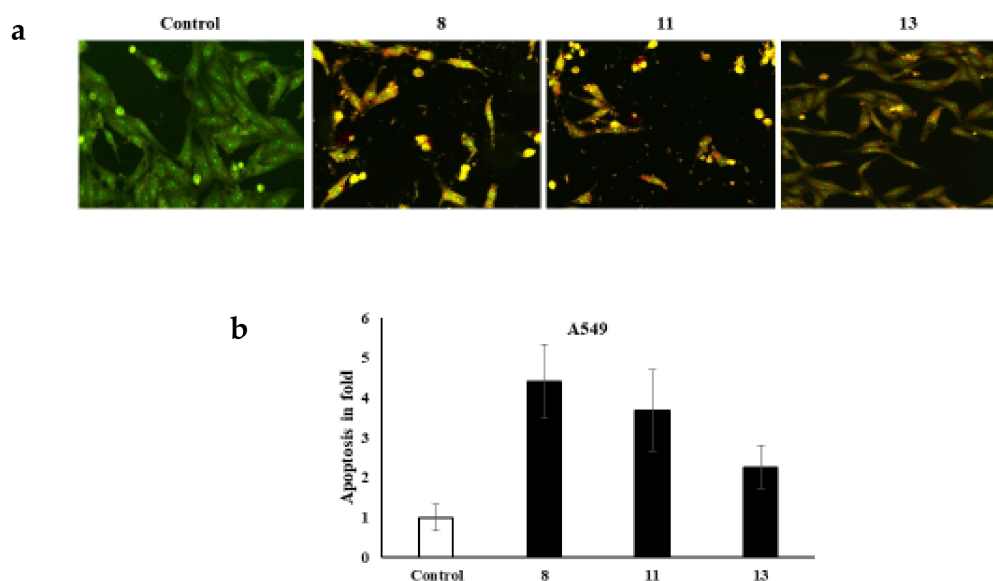


**Figure 2.** (a) dual staining of A549 cells via the fluorescent homidium bromide and acridine orange dyes; (b) apoptosis in fold.

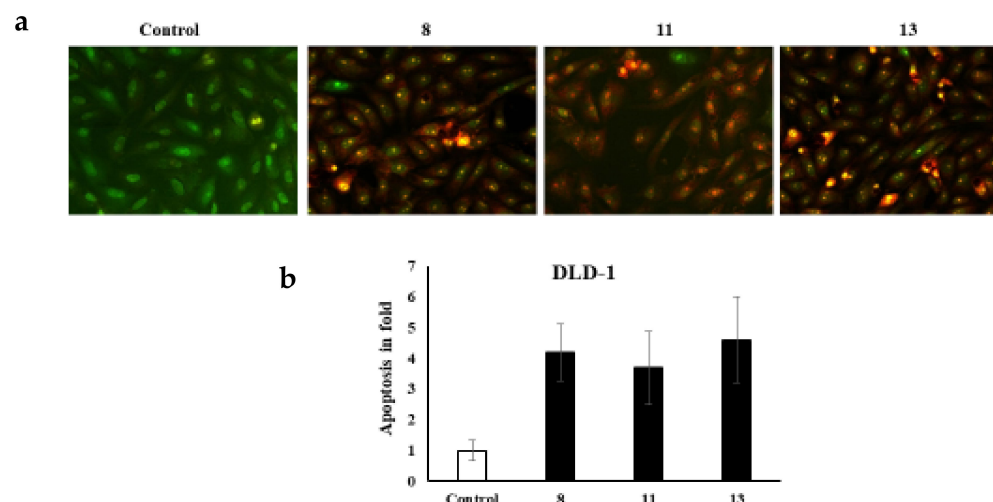


**Figure 3.** (a) dual staining of DLD-1 cells via the fluorescent homidium bromide and acridine orange dyes; (b) apoptosis in fold.

#### 4. Conclusions

This article described the design, synthesis, and biological studies of a novel series of azothiazoles based on hydrazonoyl halides. The explanation of the reaction can be through a nucleophilic substitution reaction that starts with the halogen atom from hydrazonoyl halides being replaced by the thiol nucleophile of 2-(3,4-dimethoxybenzylidene)hydrazine-1-carbothioamide (1) to form an S-alkylated intermediate. This intermediate could undergo cyclization carried out via nucleophilic addition followed by the loss of water, which would afford a novel series of azothiazoles. These reactions are provided the desired products in excellent yields. FTIR, MS, and NMR spectra elucidated structures of the final products. The new series of benzothiazoles were investigated for their potential anticancer activities and evaluated the potency of the titled compounds to promote apoptosis.

**Author Contributions:** A.R.S., H.E., S.S., S.M.G. and Y.S.A.-F.: supervision, investigation, methodology, resources, formal analysis, data curation, funding acquisition, writing—original draft, and writing—review and editing. All authors have read and agreed to the published version of the manuscript.

**Funding:** This work was supported through the Annual Funding track by the Deanship of Scientific Research, Vice Presidency for Graduate Studies and Scientific Research, King Faisal University, Saudi Arabia (Project No. GRANT680).

**Institutional Review Board Statement:** Not applicable.

**Informed Consent Statement:** Not applicable.

**Data Availability Statement:** The raw/processed data generated in this work are available upon request from the corresponding author.

**Conflicts of Interest:** The authors declare that they have no known competing financial interests or personal relationships that could have appeared to influence the work reported in this paper.

## References

1. Chankhanittha, T.; Somaudon, V.; Watcharakitti, J.; Piyavarakorn, V.; Nanan, S. Performance of solvothermally grown Bi<sub>2</sub>MoO<sub>6</sub> photocatalyst toward degradation of organic azo dyes and fluoroquinolone antibiotics. *Mater. Lett.* **2020**, *258*, 126764. [[CrossRef](#)]
2. Gaffer, H.E. Antimicrobial sulphonamide azo dyes. *Color. Technol.* **2019**, *135*, 484–500. [[CrossRef](#)]
3. Ghasemi, Z.; Azizi, S.; Salehi, R.; Kafil, H.S. Synthesis of azo dyes possessing N-heterocycles and evaluation of their anticancer and antibacterial properties. *Monatsh. Chem.* **2018**, *149*, 149–157. [[CrossRef](#)]
4. Afifi, T.H.; Okasha, R.M.; Ahmed, H.E.; Ilaš, J.; Saleh, T.; Abd-El-Aziz, A.S. Structure-activity relationships and molecular docking studies of chromene and chromene based azo chromophores: A novel series of potent antimicrobial and anticancer agents. *EXCLI J.* **2017**, *16*, 868–902. [[CrossRef](#)] [[PubMed](#)]
5. Gaffer, H.E.; Elgohary, M.R.; Etman, H.A.; Shaaban, S. Antibacterial evaluation of cotton fabrics by using novel sulfonamide reactive dyes. *Pigm. Resin Technol.* **2017**, *46*, 210–217. [[CrossRef](#)]
6. Krehl, S.; Loewinger, M.; Florian, S.; Kipp, A.P.; Banning, A.; Wessjohann, L.A.; Brauer, M.N.; Iori, R.; Esworthy, R.S.; Chu, F.F.; et al. Glutathione peroxidase-2 and selenium decreased inflammation and tumors in a mouse model of inflammation-associated carcinogenesis whereas sulforaphane effects differed with selenium supply. *J. Carcinog.* **2012**, *33*, 620–628. [[CrossRef](#)] [[PubMed](#)]
7. Gilfillan, L.; Artschwager, R.; Harkiss, A.H.; Liskamp, R.M.; Sutherland, A. Synthesis of pyrazole containing alpha-amino acids via a highly regioselective condensation/aza-Michael reaction of  $\beta$ -aryl  $\alpha,\beta$ -unsaturated ketones. *Org. Biomol. Chem.* **2015**, *13*, 4514–4523. [[CrossRef](#)] [[PubMed](#)]
8. Kantar, C.; Akal, H.; Kaya, B.; Islamoğlu, F.; Türk, M.; Şaşmaz, S. Novel phthalocyanines containing resorcinol azo dyes; synthesis, determination of pK<sub>a</sub> values, antioxidant, antibacterial and anticancer activity. *J. Organomet. Chem.* **2015**, *783*, 28–39. [[CrossRef](#)]
9. Cai, R.; Wang, D.; Chen, Y.; Yan, W.; Geise, N.R.; Sharma, S.; Li, H.; Petersen, J.L.; Li, M.; Shi, X. Facile synthesis of fluorescent active triazapentalenes through gold-catalyzed triazole-alkyne cyclization. *Chem. Commun.* **2014**, *50*, 7303–7305. [[CrossRef](#)]
10. Hamidian, H.; Tagizadeh, R.; Fozooni, S.; Abbasalipour, V.; Taheri, A.; Namjou, M. Synthesis of novel azo compounds containing 5(4H)-oxazolone ring as potent tyrosinase inhibitors. *Bioorganic Med. Chem.* **2013**, *21*, 2088–2092. [[CrossRef](#)]
11. Benkhaya, S.; M'rabet, S.; El Harfi, A. Classifications, properties, recent synthesis and applications of azo dyes. *Heliyon* **2020**, *6*, e03271. [[CrossRef](#)] [[PubMed](#)]
12. Raslan, M.A. Efficient synthesis of some new 1,3,4-Thiadiazole and thiazole derivatives via thiosemicarbazone derivatives. *Heterocycles* **2020**, *100*, 809–822. [[CrossRef](#)]
13. Sayed, A.R.; Ahmed, M.S.M.; Gomha, S.M. Efficient Methods for the Synthesis of Novel Arylazothiazoles Based on Acetylferrocene or Adamantane. *Curr. Org. Synth.* **2020**, *17*, 282–287. [[CrossRef](#)] [[PubMed](#)]
14. Farghaly, T.A.; Abo Alnaja, A.M.; El-Ghamry, H.A.; Shaaban, M.R. Synthesis and DNA binding of novel bioactive thiazole derivatives pendent to N-phenylmorpholine moiety. *Bioorg. Chem.* **2020**, *102*, 104103. [[CrossRef](#)] [[PubMed](#)]
15. Abdel Latif, N.A.; Abbas, E.M.H.; Farghaly, T.A.; Awad, H.M. Synthesis, Characterization, and Anticancer Screening of Some New Bithiazole Derivatives. *Russ. J. Org. Chem.* **2020**, *56*, 1096–1107. [[CrossRef](#)]
16. Zaki, Y.H.; Abdelhamid, A.O.; Sayed, A.R.; Mohamed, H.S. Synthesis of 1,3,4-Thiadiazole Derivatives Using Hydrazonoyl Bromide: Molecular Docking and Computational Studies. *Polycycl. Aromat. Compd.* **2022**. [[CrossRef](#)]
17. Al-Shihry, S.S.; Sayed, A.R.; Abd El-Lateef, H.M. Design and assessment of a novel poly(urethane-semicarbazides) containing thiadiazoles on the backbone of the polymers as inhibitors for steel pipelines corrosion in CO<sub>2</sub>-saturated oilfield water. *J. Mol. Struct.* **2020**, *1201*, 127223. [[CrossRef](#)]
18. Sayed, A.R.; Al-Faiyz, Y.S. convenient methods for the synthesis of novel thiadiazoles and polythiadiazoles. *Heterocycles* **2020**, *100*, 955–963. [[CrossRef](#)]
19. Abeer, M.E.; Maher, A.E.; Eslam, B.E. Eco-friendly sequential one-pot synthesis, molecular docking, and anticancer evaluation of arylidene-hydrazinyl-thiazole derivatives as CDK2 inhibitors. *Bioorg. Chem.* **2021**, *108*, 104615. [[CrossRef](#)]

20. Abd El-Lateef, H.M.; Sayed, A.R.; Shalabi, K. Synthesis and theoretical studies of novel conjugated polyazomethines and their application as efficient inhibitors for C1018 steel pickling corrosion behavior. *Surf. Interfaces* **2021**, *23*, 101037. [[CrossRef](#)]
21. Ali, S.H.; Sayed, A.R. Review of the synthesis and biological activity of thiazoles. *Synth. Commun.* **2021**, *51*, 670–700. [[CrossRef](#)]
22. Abd El-Lateef, H.M.; Sayed, A.R.; Shalabi, K. Studying the effect of two isomer forms thiazole and thiadiazine on the inhibition of acidic chloride-induced steel corrosion: Empirical and Computer simulation explorations. *J. Mol. Liq.* **2022**, *356*, 119044. [[CrossRef](#)]
23. Bakir, E.M.; Sayed, A.R.; Abd El-Lateef, H.M. Colorimetric detection of Hg<sup>2+</sup> ion using fluorescein/thiourea sensor as a receptor in aqueous medium. *J. Photochem. Photobiol. A Chem.* **2022**, *422*, 113569. [[CrossRef](#)]
24. Sayed, A.R.; Al-Faiyz, Y.S.; Elsaywy, H.; Shaaban, S.; Mohamed, M.A. Synthesis and Biochemical Studies of Novel Mon-Azothiazoles and Bis-Azothiazoles Based on 2-(4-(Dimethylamino)Benzylidene)Hydrazine-1-Carbothioamide. *Polycycl. Aromat. Compd.* **2022**. [[CrossRef](#)]
25. Samarghandi, M.R.; Zarrabi, M.; Sepehr, M.N.; Amrane, A.; Safari, G.H.; Bashiri, S. Application of acidic treated pumice as an adsorbent for the removal of azo dye from aqueous solutions: Kinetic, equilibrium and thermodynamic studies. *Iran. J. Environ. Health Sci. Eng.* **2012**, *9*, 9. [[CrossRef](#)]
26. Pinheiro, H.M.; Touraud, E.; Thomas, O. Aromatic amines from azo dye reduction: Status review with emphasis on direct UV spectrophotometric detection in textile industry wastewaters. *Dyes Pigment.* **2004**, *61*, 121–139. [[CrossRef](#)]
27. Chung, K.T.; Cerniglia, C.E. Mutagenicity of azo dyes: Structure-activity relationships. *Mutat. Res. Genet. Toxicol.* **1992**, *277*, 201–220. [[CrossRef](#)]
28. Harrington-Brock, K.; Parker, L.; Doerr, C.; Cimino, M.C.; Moore, M.M. Analysis of the genotoxicity of anthraquinone dyes in the mouse lymphoma assay. *Mutagenesis* **1991**, *6*, 35–46. [[CrossRef](#)]
29. Shaaban, S.; Negm, A.; Ashmawy, A.M.; Ahmed, D.M.; Wessjohann, L.A. Combinatorial synthesis, in silico, molecular and biochemical studies of tetrazole-derived organic selenides with increased selectivity against hepatocellular carcinoma. *Eur. J. Med. Chem.* **2016**, *122*, 55–71. [[CrossRef](#)]
30. Nury, T.; Zarrouk, A.; Vejux, A.; Doria, M.; Riedinger, J.M.; Delage-Mourroux, R.; Lizard, G. Induction of oxiaoptophagy, a mixed mode of cell death associated with oxidative stress, apoptosis and autophagy, on 7-ketocholesterol-treated 158N murine oligodendrocytes: Impairment by  $\alpha$ -tocopherol. *Biochem. Biophys. Res. Commun.* **2014**, *446*, 714–719. [[CrossRef](#)]
31. Kassab, K. Evaluating the antitumor activity of combined photochemotherapy mediated by a meso-substituted tetracationic porphyrin and adriamycin. *Acta Biochim. Biophys. Sin.* **2009**, *41*, 892–899. [[CrossRef](#)] [[PubMed](#)]
32. Zarrouk, A.; Vejux, A.; Nury, T.; El Hajj, H.I.; Haddad, M.; Cherkaoui-Malki, M.; Riedinger, J.M.; Hammami, M.; Lizard, G. Induction of mitochondrial changes associated with oxidative stress on very long chain fatty acids (C22:0, C24:0, or C26:0)-treated human neuronal cells (SK-NB-E). *Oxid. Med. Cell. Longev.* **2012**, *2012*, 623257. [[CrossRef](#)] [[PubMed](#)]
33. Vigilanza, P.; Aquilano, K.; Rotilio, G.; Ciriolo, M.R. Transient cytoskeletal alterations after SOD1 depletion in neuroblastoma cells. *Cell. Mol. Life Sci.* **2008**, *65*, 991–1004. [[CrossRef](#)] [[PubMed](#)]
34. Aydin, H.H.; Celik, H.A.; Deveci, R.; Terzioglu, E.; Karacali, S.; Mete, N.; Akarca, U.; Batur, Y. Characterization of the cellular response during apoptosis induction in cadmium-treated Hep G2 human hepatoma cells. *Biol. Trace Elem. Res.* **2003**, *95*, 139–153. [[CrossRef](#)]
35. Abd El-Lateef, H.M.; Shaaban, S.; Shalabi, K.; Khalaf, M.M. Novel organoselenium-based N-mealanilic acids as efficacious corrosion inhibitors for 6061 aluminum alloy in molar HCl: In-silico modeling, electrochemical, and surface morphology studies. *J. Taiwan Inst. Chem. Eng.* **2022**, *133*, 104258. [[CrossRef](#)]
36. Li, B.; Li, W.; Tian, Y.; Guo, S.; Qian, L.; Xu, D.; Cao, N. Selenium-Alleviated Hepatocyte Necrosis and DNA Damage in Cyclophosphamide-Treated Geese by Mitigating Oxidative Stress. *Biol. Trace Elem. Res.* **2020**, *193*, 508–516. [[CrossRef](#)]
37. Elmore, S. Apoptosis: A review of programmed cell death. *Toxicol. Pathol.* **2007**, *35*, 495–516. [[CrossRef](#)]
38. Wang, X.; Zhong, X.; Li, J.; Liu, Z.; Cheng, L. Inorganic nanomaterials with rapid clearance for biomedical applications. *Chem. Soc. Rev.* **2021**, *50*, 8669–8742. [[CrossRef](#)]
39. Miao, Z.; Chen, S.; Xu, C.-Y.; Ma, Y.; Qian, H.; Xu, Y.; Chen, H.; Wang, X.; He, G.; Lu, Y.; et al. PEGylated rhenium nanoclusters: A degradable metal photothermal nanoagent for cancer therapy. *Chem. Sci.* **2019**, *10*, 5435–5443. [[CrossRef](#)]
40. Wang, X.; Yue, Q.; Xu, H.; Zhong, X.; Sun, L.; Li, G.; Gong, Y.; Yang, N.; Wang, Z.; Liu, Z.; et al. Liquid exfoliation of TiN nanodots as novel sonosensitizers for photothermal-enhanced sonodynamic therapy against cancer. *Nano Today* **2021**, *39*, 101170. [[CrossRef](#)]
41. Zhong, X.; Wang, X.; Li, J.; Hu, J.; Cheng, L.; Yang, X. ROS-based dynamic therapy synergy with modulating tumor cell-microenvironment mediated by inorganic nanomedicine. *Coord. Chem. Rev.* **2021**, *437*, 213828. [[CrossRef](#)]